REFINEMENT OF Mn-SUBSTITUTED MUSCOVITE AND PHLOGOPITE

Rick A. Knurr and S. W. Bailey

Department of Geology and Geophysics, University of Wisconsin–Madison
Madison, Wisconsin 53706

Abstract—The crystal structures of a reddish-purple, Mn-bearing muscovite-$2M_1$ (alurgite variety) and a reddish-brown, Mn-bearing phlogopite-$1M$ (manganophyllite variety) were refined to final residuals of 2.7% and 3.1%, respectively. The refinements were carried out in space groups $C2/c$ and $C1$ for alurgite and $C2/m$ and $C2$ for manganophyllite. The $C1$ and $C2$ subgroup refinements gave atomic coordinates consistent with the parent space group refinements. No cation ordering was found in either specimen, and the structures are very similar to those of muscovite and phlogopite. Residual areas of positive electron densities were found between the tetrahedral cations and neighboring oxygens in difference maps of both minerals. Those of alurgite were examined in detail to show the correlation between the residual densities and covalent bonding in the tetrahedra. The valence of the Fe present was determined by Mössbauer spectra as Fe^{3+} in both samples and of the Mn by optical spectra as Mn^{3+} in the alurgite but as Mn^{2+} in the manganophyllite.

Key Words—Alurgite, Crystal structure, Manganese, Manganophyllite, Muscovite, Phlogopite.

INTRODUCTION

Several workers (Penfield, 1893; Bilgrami, 1956; Heinrich and Levinson, 1955) have referred to a red to purple variety of muscovite called alurgite (from the Greek word for purple). The mineral was named by Breithaupt in 1865 and was first characterized in detail by Penfield (1893). Penfield's wet chemical analysis (in weight percentages) (53.22 SiO_2, 21.19 Al_2O_3, 1.22 Fe_2O_3, 0.87 Mn_2O_3, 0.18 MnO, 6.02 MgO, 11.20 K_2O, 0.34 Na_2O, 5.75 H_2O) showed that alurgite from St. Marcel, Italy, contained small amounts of manganese and iron and was Si-rich. Surprisingly, the structure of alurgite was described by Penfield at that time as being closely related to that of lepidolite. Heinrich and Levinson (1955) showed later that alurgite is closely related to muscovite in structure and chemistry, although some specimens may be phengitic. A less deeply colored Mn-bearing dioctahedral mica has been called rose muscovite. This mica also is essentially isostructural with muscovite. Its chemistry shows little variation in SiO_2 and Al_2O_3 from that of pure muscovite. It has cell dimensions similar to muscovite and occurs as the $2M_1$ polytype (Heinrich and Levinson, 1953). The iron content is very low and total manganese is also low. Rose muscovite differs from alurgite primarily in color rather than in bulk chemistry.

Manganophyllite is a trioctahedral Mn-bearing mica. According to Heinrich (1946) and Heinrich and Levinson (1953), most specimens that have been called manganophyllite have only small amounts of Fe relative to Mg and should be classified as a variety of phlogopite. The less abundant Fe^{2+}-rich specimens may be classified as manganoan biotites. Literature values of the manganese contents of manganophyllites are ex-

tremely variable. Jakob (1925) reported specimens with as much as 18 weight percent total manganese oxide, but values generally range from 1 to 10 weight percent. Like phlogopite, manganophyllite occurs primarily as the $1M$ polytype. Its color has been described variously as copper-red to bronze to red-brown making it, like alurgite, a distinctive mineral in appearance.

Attempts to synthesize pure trioctahedral Mn-micas have been unsuccessful (Hazen and Wones, 1972). The failure has been attributed to the large radius of the divalent Mn cation (0.83 Å) that, when incorporated in the phlogopite structure, enlarges the octahedra and creates severe lateral misfit between the tetrahedral and octahedral sheets. The smaller Mn^{3+} cation (0.645 Å radius) is more easily incorporated into the structure, but is not considered a particularly stable cation because it has four unpaired 3d electrons as compared to the more stable state of five unpaired 3d electrons in the divalent ion. Burns (1970, p. 59) suggested from absorption spectrum data, however, that the distorted octahedral site of the phlogopite structure may stabilize the Mn^{3+} cation.

The Mn-bearing micas alurgite and manganophyllite are found in metamorphosed sedimentary manganese deposits. The degree of metamorphism appears to be extremely variable but generally entails at least medium pressure and medium temperature. The most common reported occurrences of these micas are in the manganese deposits of India, Sweden, and Brazil. The manganophyllite sample used in this study came from Langban, Sweden, and the alurgite sample from Minas Gerais, Brazil. Both specimens were obtained from Minerals Unlimited.

This study was initiated originally to determine the

7

Table 1. Microprobe analyses of alurgite and manganophyllite.

	Alurgite (Minas Gerais, Brazil)		Manganophyllite (Langban, Sweden)	
	Wt. %	Atoms[2]	Wt. %	Atoms
SiO_2	45.19	3.055	39.23	2.790
Al_2O_3	33.42	0.945 / 1.718	15.79	1.210 / 0.114
MgO	0.98	0.099	23.64	2.506
Fe_2O_3[1]	2.92	0.149	3.23	0.173
Mn_2O_3[1]	0.39	0.020	—	—
MnO	—	—	2.69	0.132
Cr_2O_3	0.00	0.000	n.a.	—
TiO_2	0.45	0.023	0.17	0.009
K_2O	10.79	0.930	9.30	0.844
Na_2O	0.40	0.052	0.49	0.068
CaO	0.00	0.000	0.02	0.002
BaO	0.23	0.007	0.06	0.017
F	n.a.	—	0.43	0.097
Cl	0.00	0.000	0.00	0.000

[1] Valence determined by Mössbauer or optical spectra.
[2] Per $O_{10}(OH)_2$.

effect of Mn-substitution on the basic structures of muscovite and phlogopite and to explain the striking color differences observed in the two specimens. Early in the investigation electron microprobe analysis showed that very little of the chromophoric element was apparently necessary to produce the characteristic colors in either alurgite or manganophyllite; the concentration of both Mn and Fe in the specimens under study proved to be less than 0.2 atoms per formula unit, thus negating any appreciable structural effects due to their presence. In the interim, a structural analysis of two manganophyllite specimens containing substantially more Mn than our specimen was published (Guggenheim and Kato, 1984), and an optical and Mössbauer spectra study relating to the pleochroism and color of Mn-micas was published by Smith et al. (1983). Thus, the structural refinements of the present study were directed towards the detection of possible octahedral cation ordering in subgroup symmetry and towards the determination of the significance of residual peaks observed on difference electron-density maps.

EXPERIMENTAL

Untwinned single crystals of alurgite and manganophyllite showing sharp optical extinction were selected from the samples. The alurgite crystal measured $0.26 \times 0.57 \times 0.20$ mm and was deep reddish-purple in plain light. The crystal of manganophyllite measured $0.58 \times 0.70 \times 0.15$ mm and was dark red-brown in plain light. Both crystals showed normal pleochroism in polarized light. Electron microprobe analyses and corresponding structural formulae (based on 11 oxygens) are given in Table 1.

Preliminary precession photographs showed manganophyllite to occur as the $1M$ polytype and alurgite

as the $2M_1$ polytype. Both were shown to possess C-centered lattices. Unit-cell dimensions were determined by least squares refinement of 15 reflections for alurgite and 12 reflections for manganophyllite. The cell dimensions calculated for alurgite were $a = 5.2044(8)$ Å, $b = 9.018(2)$ Å, $c = 20.073(5)$ Å, $\beta = 95.82(2)°$, and those for manganophyllite were $a = 5.316(1)$ Å, $b = 9.221(4)$ Å, $c = 10.282(4)$ Å, and $\beta = 99.90(3)°$.

Reflection intensities were measured in all eight octants of the limiting sphere to $2\theta = 60°$ on a Nicolet $P2_1$ automated single-crystal diffractometer with graphite-monochromatized $MoK\alpha$ radiation. The data were collected in the $2\theta{:}\theta$ variable scan mode. One standard reflection was checked after every 50 reflections to monitor electronic and crystal stability. Reflections were considered observed if $I > 2\sigma(I)$. Integrated intensity I was calculated from $I = [S - (B_1 + B_2)/B_r]T_r$, where S is the scan count, B_1 and B_2 the backgrounds, B_r the ratio of background time to scan time, and T_r the 2θ scan rate in °/min. Values of $\sigma(I)$ were calculated from standard counting statistics. Integrated intensities were corrected for Lorentz and polarization factors. Absorption corrections were made by the empirical ψ-scan method.

REFINEMENT

The X-ray diffraction data set for alurgite consisted of 5539 reflections, which yielded 1280 independent reflections when merged in monoclinic symmetry. Sixteen apparent violations of monoclinic symmetry equivalence and 8 violations of c-glide extinctions (plus Friedel equivalents) were recorded. Starting atomic positions for a $2M_1$ muscovite were taken from Rothbauer (1971). A total of 1261 reflections was refined in $C2/c$ symmetry using the least squares program ORFLS. Scattering factors from Cromer and Mann (1968) appropriate for 50% ionization were used for both alurgite and manganophyllite in the refinement process. Unit weights were used in both refinements because experience in this laboratory has shown them to be superior to sigma weights for the intensity distributions found in layer silicate minerals. Refinement of atomic coordinates and anisotropic thermal parameters of alurgite resulted in an unweighted residual of 0.028. The hydrogen proton of the OH group then was located on a difference electron density map in which the extra peak for hydrogen represented 0.45 electrons/ $Å^3$. The hydrogen was included in the structure at this stage, but none of its parameters were varied. The final cycles of refinement reduced R to 0.027. Final coordinates and temperature factors are found in Table 2. Table 3 gives the orientations of the anisotropic thermal ellipsoids relative to the crystallographic axes.

A refinement in triclinic symmetry also was attempted to test the significance of the apparent monoclinic and c-glide violations. The violating reflections were

Table 2.   Final coordinates and temperature factors of alurgite and manganophyllite.

	x	y	z	B(equiv)[1]	Beta(1,1)	Beta(2,2)	Beta(3,3)	Beta(1,2)	Beta(1,3)	Beta(2,3)
Alurgite										
T(1)	.4650(1)	.92992(7)	.13554(3)	0.668	.0048(2)	.00204(7)	.00052(1)	-.00001(9)	.0035(4)	.00006(3)
T(2)	.4514(1)	.25874(8)	.13556(3)	0.664	.0046(2)	.00213(7)	.00051(1)	.0001(1)	.00027(4)	.00003(3)
M(2)	.2498(1)	.08320(8)	.00004(4)	0.551	.0033(2)	.00183(7)	.00044(1)	-.00009(9)	.00029(4)	.00006(3)
K	.0000	.0988(1)	.25000	1.895	.0175(3)	.0062(1)	.00112(2)	.00000	.00061(6)	.00000
O(1)	.4616(3)	.9437(2)	.05368(9)	0.977	.0078(6)	.0034(2)	.00062(4)	.0004(3)	.0004(1)	.00006(7)
O(2)	.3853(3)	.2518(2)	.05373(9)	0.957	.0089(6)	.0030(2)	.00059(4)	-.0001(3)	.0004(1)	.00011(7)
O(3)	.4195(4)	.0933(2)	.16851(9)	1.349	.0149(7)	.0036(2)	.00081(4)	.0004(3)	.0009(1)	-.00002(8)
O(4)	.2489(4)	.8126(2)	.1577(1)	1.485	.0108(6)	.0054(2)	.00097(5)	-.0015(3)	.0001(1)	.00050(8)
O(5)	.2484(4)	.3692(2)	.1689(1)	1.324	.0105(6)	.0047(2)	.00083(4)	.0016(3)	.0003(1)	-.00017(8)
O(6)	.4576(3)	.5621(2)	.05076(9)	1.131	.0094(6)	.0036(2)	.00076(4)	-.0003(3)	.0008(1)	-.00024(7)
H	.3792	.6505	.0595	2.0						
Manganophyllite										
T(1)	.0754(1)	.33318(8)	.22758(7)	0.701	.0035(2)	.00203(7)	.00251(6)	.0000(1)	.00095(8)	.00003(5)
M(1)	.00000	.50000	.50000	0.989	.0052(4)	.0027(1)	.0036(1)	.00000	.0013(2)	.00000
M(2)	.00000	.1680(1)	.50000	0.902	.0042(3)	.0026(1)	.00332(9)	.00000	.0009(1)	.00000
K	.00000	.00000	.00000	2.351	.0206(5)	.0077(2)	.0053(1)	.00000	.0019(2)	.00000
O(1)	.3321(4)	.2753(2)	.1703(2)	1.480	.0102(6)	.0053(2)	.0037(2)	.0021(3)	.0022(2)	.0007(2)
O(2)	.06656(6)	.50000	.1709(3)	1.435	.0145(9)	.0034(3)	.0038(2)	.00000	-.0002(4)	.00000
O(3)	.1302(3)	.3331(2)	.3817(2)	0.975	.0057(5)	.0029(2)	.0032(2)	-.0001(3)	.0011(2)	.0001(1)
O(4)	.1392(5)	.00000	.3993(9)	0.989	.0062(7)	.0031(3)	.0030(2)	.00000	.0009(3)	.00000
H	.12(2)	.00000	.325(9)	2.0						

[1] $B(equiv) = 4/3(Beta(1,1)/(a^*)^2 + Beta(2,2)/(b^*)^2 + Beta(3,3)/(c^*)^2)$.

Table 3. Thermal ellipsoid orientations in alurgite and manganophyllite.

Atom	Axis	Alurgite RMS (Å) displacement	Angle (°) with respect to X	Y	Z	Manganophyllite RMS (Å) displacement	Angle (°) with respect to X	Y	Z
K	r1	0.149(1)	58(9)	90(0)	154(9)	0.166(2)	69(26)	90(0)	169(26)
	r2	0.155(2)	32(10)	90(0)	64(10)	0.169(2)	21(26)	90(0)	79(26)
	r3	0.160(1)	90(0)	180(0)	90(0)	0.183(2)	90(0)	180(0)	90(0)
T(1)	r1	0.079(2)	12(4)	86(6)	107(3)	0.067(2)	177(2)	92(3)	78(1)
	r2	0.091(2)	96(6)	13(6)	101(6)	0.094(2)	92(3)	2(3)	91(3)
	r3	0.103(1)	100(3)	102(6)	160(4)	0.114(1)	92(1)	92(3)	168(1)
T(2)	r1	0.078(2)	174(3)	88(5)	79(3)	—	—	—	—
	r2	0.094(2)	89(5)	9(8)	99(8)				
	r3	0.102(1)	96(3)	99(8)	165(6)				
M(1)	r1					0.083(4)	179(2)	90(0)	79(2)
	r2	(vacant)	—	—	—	0.108(3)	90(0)	0(0)	90(0)
	r3					0.136(3)	91(2)	90(0)	169(2)
M(2)	r1	0.065(2)	170(3)	96(4)	76(3)	0.075(3)	178(2)	90(0)	82(2)
	r2	0.086(2)	98(4)	19(7)	106(7)	0.105(2)	90(0)	0(0)	90(0)
	r3	0.095(2)	96(3)	108(8)	159(6)	0.131(2)	88(2)	90(0)	172(2)
O(1)	r1	0.100(4)	20(10)	101(9)	113(13)	0.105(4)	159(3)	71(4)	71(5)
	r2	0.111(4)	79(14)	114(17)	30(15)	0.131(3)	90(6)	119(5)	30(5)
	r3	0.121(3)	107(8)	153(16)	108(16)	0.163(3)	111(3)	144(4)	113(4)
O(2)	r1	0.103(4)	58(20)	62(16)	140(14)	0.121(5)	90(0)	180(0)	90(0)
	r2	0.111(4)	23(*)	118(*)	77(*)	0.128(5)	52(7)	90(0)	48(7)
	r3	0.115(4)	102(34)	138(29)	128(16)	0.157(4)	38(7)	90(0)	138(7)
O(3)	r1	0.119(4)	65(10)	133(29)	130(26)	0.088(4)	176(8)	94(8)	80(4)
	r2	0.124(4)	106(14)	137(29)	49(26)	0.111(3)	94(8)	5(9)	93(9)
	r3	0.146(3)	150(6)	96(6)	113(6)	0.129(3)	90(4)	94(9)	169(6)
O(4)	r1	0.115(4)	154(8)	116(6)	80(10)	0.092(6)	178(7)	90(0)	83(7)
	r2	0.129(4)	72(11)	117(7)	37(5)	0.116(5)	90(0)	0(0)	90(0)
	r3	0.165(3)	71(3)	141(4)	125(4)	0.125(5)	88(7)	90(0)	173(7)
O(5)	r1	0.109(4)	31(5)	120(4)	102(8)	—	—	—	—
	r2	0.128(3)	76(8)	80(8)	22(8)				
	r3	0.148(3)	117(4)	148(4)	72(7)				
O(6)	r1	0.102(4)	35(8)	101(9)	129(6)	—	—	—	—
	r2	0.117(4)	64(10)	35(9)	71(9)				
	r3	0.135(3)	112(6)	57(8)	135(6)				

reinserted into the data set, and only the coordinates of the octahedral cations and their coordinating anions were varied in subgroup $C1$. The resulting triclinic atomic positions were found to be within 3σ of the monoclinic positions; most of them were within 1σ. These results suggest that the violations do not constitute a large enough deviation from the monoclinic set to enable refinement in the lower symmetry.

The data set for manganophyllite consisted of 2922 reflections, which yielded 719 independent reflections when merged in monoclinic symmetry. Thirty-four apparent violations of monoclinic equivalence were recorded. Atomic positions for phlogopite-$1M$ were taken from Joswig (1972) for starting parameters. A total of 685 reflections was refined initially in the ideal space group $C2/m$. Refinement using unit weights and anisotropic temperature factors produced an unweighted residual of 0.049. At this point it was noticed that the structure amplitudes of several low-angle reflections varied considerably from those calculated. Three reflections were excluded from the data set after being identified as suffering extinction effects, and 13 others were excluded after inspection of film data indicated possible streaking effects. Subsequent refinement reduced R to 0.034. A difference electron density map was used to locate the hydrogen proton of the OH group, which gave a positive peak of 0.5 electron/$Å^3$. Final coordinates, thermal parameters, and thermal ellipsoid orientations for manganophyllite are reported in Tables 2 and 3.

A refinement in subgroup symmetry $C2$ was attempted for manganophyllite because of communication with S. Guggenheim (Department of Geological Sciences, University of Illinois at Chicago) who had found a weak, positive acentric signal on a different sample of manganophyllite from the same locality using a second harmonic generation (SHG) analysis (see Guggenheim *et al.*, 1983; sample 11, in Table 1). In the
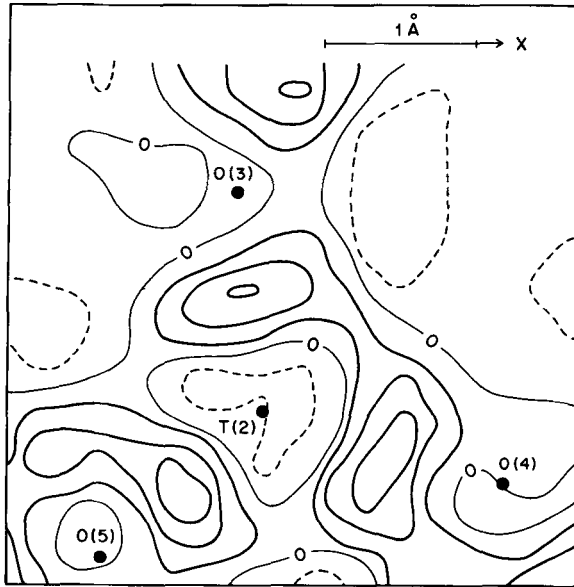
Figure 1. Electron density difference map of alurgite-$2M_1$ on section parallel to XY plane at z-level halfway between T(2) and its basal oxygens. Contours are at intervals of 0.1 electrons.

Figure 2. Detailed graph of shapes of residual electron densities observed on difference maps of alurgite-$2M_1$ for bonds between T(2) and its four coordinating anions.

choice of the subgroup symmetry $C2$, we decided that octahedral ordering was more probable than tetrahedral ordering and that removal of the mirror plane would be the most probable result from ordering in the M(2) octahedral sites. Two octahedral ordering patterns were postulated, and their ideal atomic positions were determined by use of the distance-least-squares program OPTDIS (Dollase, 1980). The two octahedra related by the mirror plane in $C2/m$ symmetry were labeled M(2) and M(22). Ordering arrangement 1 postulated M(22) to be larger than M(2), and ordering arrangement 2, the reverse. In both arrangements the tetrahedra were assumed to be disordered, and the origin was defined by holding the potassium atom constant in position.

Both ordering schemes were refined as far as possible, including use of anisotropic temperature factors. The resulting bond lengths from the refinement for arrangement 1 suggested an ordering scheme opposite to that of the input model. Arrangement 2 refinement gave bond lengths suggestive of a disordered cation distribution and also produced one 'not-positive-definite' temperature factor. Coordinate comparison showed that the $C2$ refinements of both ordering models gave atomic coordinates that were within three standard deviations of those from the $C2/m$ refinement. The $C2/m$ symmetry is thus the best approximation for the structure, but small deviations from monoclinic symmetry and from centrosymmetry may have given the observed 34 violations of monoclinic symmetry and the weak SHG signal. Similar conclusions were
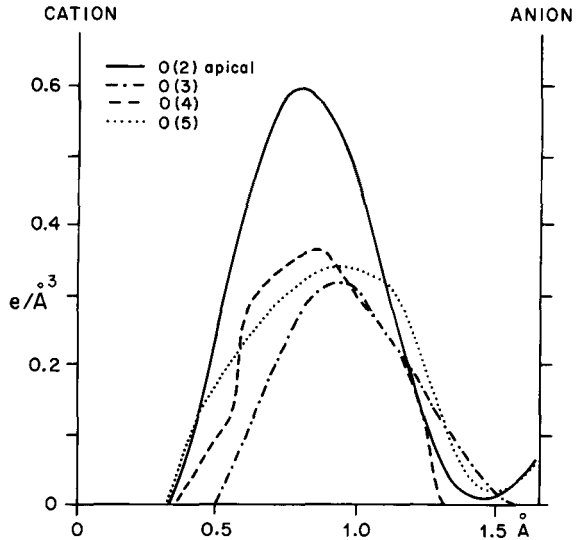
reached by Guggenheim and Kato (1984) for their specimens. The sensitivity of the SHG method to small deviations is not known. A table of final F_0 and F_c values for both structures may be obtained from the authors on request.

ELECTRON DENSITY DIFFERENCE MAPS

In the $C2/c$ refinement of alurgite, after the hydrogen atom had been included, positive areas of electron density on difference maps representing about 0.6 electrons/$Å^3$ were found between the apical oxygens and the tetrahedral cations. Further inspection located similar areas of positive electron density representing about 0.3 electrons/$Å^3$ between the tetrahedral cations and the basal oxygens. These same anomalies also were found in the difference maps of manganophyllite.

Figure 1 shows electron density contours on a difference section taken parallel to (001) and through the T(2) tetrahedron of alurgite. Between the tetrahedral cation and each of the basal oxygens is an area of positive electron density of about 0.30–0.40 electrons/$Å^3$ that represents a departure from the proposed structure. Similar tetrahedral residual peaks were reported by Sasaki et al. (1980), Fujino et al. (1981), and Gibbs (1982) and were attributed to covalent bonding between the oxygens and the cation (Al or Si). To investigate the phenomenon further, Fourier difference map sections were calculated along T–O bonds in alurgite, and the resulting electron densities (about 15 data points per bond) were plotted against distance from the cation to the anion. This procedure was carried out for all four tetrahedral bonds with the results as shown in Figure 2. The resulting curves are roughly symmetrical, and the maxima are near the center of the bonds. A

Table 4. Bond lengths and angles of alurgite and manganophyllite.

Alurgite

T(1)–O(1)*	1.646(2) Å	T(2)–O(2)*	1.645(2) Å
–O(3)	1.643(2)	–O(3)	1.647(2)
–O(4)	1.638(2)	–O(4)	1.640(2)
–O(5)	1.650(2)	–O(5)	1.644(2)
Mean	1.644(1)	Mean	1.644(1)
O(1)–O(3)	2.699(3) Å	O(2)–O(3)	2.702(3) Å
–O(4)	2.729(3)	–O(4)	2.727(3)
–O(5)	2.707(3)	–O(5)	2.704(3)
O(3)–O(4)	2.685(3)	O(3)–O(4)	2.641(3)
–O(5)	2.648(3)	–O(5)	2.643(3)
O(4)–O(5)	2.636(3)	O(4)–O(5)	2.687(3)
Mean	2.684(1)	Mean	2.684(1)
O(3)–T(1)–O(4)	109.8(1)°	O(3)–T(2)–O(4)	106.9(1)°
O(3)–T(1)–O(5)	107.1(1)	O(3)–T(2)–O(5)	106.9(1)
O(3)–T(1)–O(1)	110.3(1)	O(3)–T(2)–O(2)	110.3(1)
O(4)–T(1)–O(1)	112.4(1)	O(4)–T(2)–O(2)	112.2(1)
O(4)–T(1)–O(5)	106.6(1)	O(4)–T(2)–O(5)	109.8(1)
O(5)–T(1)–O(1)	110.4(1)	O(5)–T(2)–O(2)	110.6(1)
Mean	109.4(1)	Mean	109.5(1)

M(2)–O(1)	1.928(2) Å
–O(1)	1.951(2)
–O(2)	1.927(2)
–O(2)	1.953(2)
–O(6)	1.923(2)
–O(6)	1.923(2)
Mean	1.934(1)

Unshared lateral		Shared diagonal	
O(1)–O(2)	2.807(3) Å	O(1)–O(1)	2.452(4) Å
	2.803(2)	O(2)–O(2)	2.453(4)
O(1)–O(6)	2.800(3)	O(6)–O(6)	2.405(4)
	2.827(3)	Mean	2.437(2)
O(2)–O(6)	2.803(3)		
	2.825(3)		
Mean	2.811(1)		
Unshared diagonal		Vacant unshared lateral	
O(1)–O(2)	2.956(3) Å	O(1)–O(2)	3.463(2) Å
O(1)–O(6)	2.869(3)	O(1)–O(6)	3.442(3)
O(2)–O(6)	2.869(3)	O(2)–O(6)	3.441(3)
Mean	2.898(2)	Mean	3.449(2)
K–O(3)	2.858(2) (2 ×) Å	H–O(6)	0.920(2) Å
–O(4)	2.893(2) (2 ×)		
–O(5)	2.866(2) (2 ×)		
Mean	2.872(1)		
K–O(3)	3.287(2) (2 ×) Å		
–O(4)	3.502(2) (2 ×)		
–O(5)	3.271(2) (2 ×)		
Mean	3.353(1)		

Manganophyllite

T(1)–O(1)	1.664(2) Å	O(1)–T(1)–O(2)	108.5(1)°
–O(1)	1.661(2)	O(1)–T(1)–O(3)	110.3(1)
–O(2)	1.663(1)	O(1)–T(1)–O(1)	108.50(8)
–O(3)*	1.662(2)	O(1)–T(1)–O(3)	110.5(1)
Mean	1.663(1)	O(2)–T(1)–O(3)	110.2(1)
		Mean	109.5(1)
O(3)–O(1)	2.731(3) Å		
–O(1)	2.730(3)		
–O(2)	2.728(3)		
O(1)–O(1)	2.699(1)		

Table 4. Continued.

–O(2)	2.700(3)		
–O(2)	2.702(2)		
Mean	2.715(1)		
M(1)–O(3)	2.087(2) (4 ×) Å		
–O(4)	2.046(3) (2 ×)		
Mean	2.783(2)		
Shared edges			
O(3)–O(4)	2.765(3) (4 ×) Å		
–O(3)	2.818(4) (2 ×)		
Mean	2.783(2)		
Unshared edges			
O(3)–O(4)	3.072(3) (4 ×) Å		
–O(3)	3.079(4) (2 ×)		
Mean	3.074(2)		
M(2)–O(3)	2.074(2) (2 ×) Å		
–O(3)	2.086(2) (2 ×)		
–O(4)	2.055(2) (2 ×)		
Mean	2.072(1)		
Shared edges			
O(3)–O(3)	2.821(4) (2 ×) Å		
	2.818(4)		
O(3)–O(4)	2.765(3)		
O(4)–O(4)	2.700(5)		
Mean	2.782(2)		
Unshared edges			
O(3)–O(3)	3.068(2) (2 ×) Å		
O(3)–O(4)	3.072(2) (2 ×)		
	3.073(3) (2 ×)		
Mean	3.071(1)		
K–O(1)	2.949(2) (4 ×) Å	H–O(4)	0.76(9) Å
–O(2)	2.952(3) (2 ×)		
Mean	2.950(1)		
K–O(1)	3.401(2) (4 ×)		
–O(2)	3.400(3) (2 ×)		
Mean	3.401(1)		

definite difference, however, exists in peak height between the apical bond curve and those of the three basal oxygens. The maximum peak heights are: T(2)–O(2) 0.60 e/Å³, T(2)–O(3) 0.32 e/Å³, T(2)–O(4) 0.36 e/Å³, and T(2)–O(5) 0.34 e/Å³. The excess electron density associated with the T–O$_{apical}$ bond is roughly twice that observed for each of the three T–O$_{basal}$ bonds as is to be expected due to the bonding of O$_{apical}$ to only one tetrahedral cation, whereas the O$_{basal}$ atoms bond to two tetrahedral cations each.

The electron density residuals shown in Figure 2 indicate to a first approximation that each basal oxygen in alurgite shares 0.68 electrons with two tetrahedral cations in partly covalent bonds such that their effective charge is reduced from -2.0 to -1.32 each, whereas the effective charge of the apical oxygen becomes -1.40. The hybrid tetrahedral cation ($Si_{0.764}Al_{0.236}$) has a formal charge of $+3.76$, which is reduced to an ef-

fective charge of $+2.14$ due to the 1.62 electrons it shares with its four oxygen neighbors. It should be noted that the effect of the interlayer potassium on the basal oxygens was ignored in this calculation because of the more ionic nature of the K–O$_{basal}$ bond. Some covalent sharing may be involved in the bonding of the octahedral cations to the apical oxygens, and calculation of the effective charge of the apical oxygens should include a correction for this effect. The uncorrected effective charges on the oxygens of -1.32 and -1.40 are in accord with the values of -1.1 to -1.5 found by more sophisticated methods by Sasaki et al. (1980) in a few other silicate minerals.

The effects of the positional disorder of tetrahedral Si,Al are not considered here nor are any possible errors due to extinction and incomplete correction for absorption by the ψ scan technique. Other smaller positive electron density residuals were noted in the vicin-

ity of the K atom in alurgite. These residuals are believed to be spurious and due to such errors or possibly to termination of series ripples. Although the latter are usually considered to be cancelled by the different Fourier method, recent detailed study suggests otherwise (G. V. Gibbs, Virginia Polytechnic Institute, personal communication, 1984). The larger residuals between the tetrahedral cations and their anions are believed to be real because of the low R values of the refinements and the consistent 2:1 ratios found between the residuals associated with the apical and basal oxygens.

MÖSSBAUER AND OPTICAL SPECTRA

Mössbauer [57]Fe spectra were obtained for each sample by W. A. Dollase (Department of Geology, University of California, Los Angeles) to determine the valence and location of the iron present. Dollase (personal communication to S.W.B., 1982) reported for each sample that the observed spectrum could be fitted with one doublet that could be assigned unambiguously to ferric iron in octahedral coordination.

	alurgite	manganophyllite
IS	0.35(3) mm/s	0.38 mm/s
		(relative to Fe metal)
QS	0.73(3) mm/s	0.94(2) mm/s
Γ	0.87(3) mm/s	0.69(2) mm/s

No ferrous doublets were observed, but the spectral noise might have obscured weak doublets representing less than 5% of the total iron. The total area under the ferric doublet of manganophyllite is 1.10 times that for the doublet of alurgite, in close agreement with the electron microprobe analyses for total iron (ratio of 1.11 from Table 1). No tetrahedral Fe was detected.

G. R. Rossman (Division of Geological and Planetary Sciences, California Institute of Technology) obtained optical spectra on both samples. Rossman (personal communication to S.W.B., 1983) reported that the Fe is trivalent in both samples, in agreement with the Mössbauer interpretation, but that the Mn is trivalent in the alurgite sample and divalent in the manganophyllite sample. The structural formulae of Table 1 were calculated on the basis of these results.

DISCUSSION

Alurgite

Table 4 shows the calculated bond lengths and angles for alurgite. The identical mean T–O bond lengths of 1.644 Å for T(1) and T(2) indicate tetrahedral cation disorder. This fact, combined with the flat difference maps at the atomic positions and the low residual of 2.7%, suggests strongly that the $C2/c$ group in which the data were refined represents the true symmetry of the structure.

The hydrogen proton of alurgite-$2M_1$ was located on difference maps at a distance of 0.92 Å from the center

of the OH group. The O...H vector points toward the vacant M(1) site in projection and is inclined at an angle of +10.9° above the surface of the octahedral sheet thereby minimizing repulsion from the interlayer cation. In muscovite-$2M_1$ Rothbauer (1971) located the hydrogen more accurately by neutron diffraction at a distance of 0.9285 Å from the center of the OH group and inclined at an angle of +12.1°. Table 5 compares several other structural features of alurgite-$2M_1$ with Rothbauer's structure of muscovite-$2M_1$. All of the values are similar.

The anisotropic thermal ellipsoids of the cations and apical oxygens are nearly isotropic. Those of the basal oxygens are larger than those of the apical oxygens due to positional disorder of the tetrahedral cations and are elongate normal to the T–O$_b$ bonds (Table 3). The directional portion of the anisotropy, as distinct from the magnitudes, thus represents true thermal vibration.

The chemical analysis of this alurgite sample (Table 1) clearly is not analogous to that of lepidolite as Penfield (1893) suggested. The $Si_{0.76}Al_{0.24}$ tetrahedral composition from Table 1 gives a Si to Al ratio of 3.2:1 that indicates a slight phengitic enrichment in Si, and is consistent with the analyses given by Heinrich and Levinson (1955) for rose muscovite and alurgite. The observed mean T–O bond length of 1.644 Å corresponds to a mean composition of $Si_{0.78}Al_{0.22}$ according to the regression equation for micas given by Hazen and Burnham (1973), in good agreement with the chemical analysis. Compositionally this alurgite corresponds well with muscovite. The only variance is the tetrahedral Si:Al ratio mentioned above, which is coupled with octahedral substitution of Mn, Fe, Mg, and Ti (a total of 0.15 atoms per site) for Al. Difference maps indicate none of the heavy elements are in tetrahedral sites. The effects of the substitutions are to increase the cell dimensions slightly, to increase the mean M(2)–O,OH bond length from 1.930 Å (for Rothbauer's structure of muscovite) to 1.934 Å, to increase slightly the octahedral sheet thickness, and to give alurgite its characteristic reddish-purple color.

The substitution of small amounts of manganese into a muscovite structure could lead to one of three varietal forms. The additions of Mn^{2+} ($\pm Fe^{2+}$, Mg^{2+}) with accompanying Si enrichment to balance the charge leads to alurgite in the Penfield sense (better described as phengite or phengitic muscovite). The addition of Mn^{3+} ($\pm Fe^{3+}$) leads either to rose muscovite or to the more deeply colored alurgite of this study. In both of these latter varieties the octahedral substitutions are primarily by trivalent cations and do not require Si enrichment. Rose muscovite and alurgite appear to be used at the present time only as varietal names, based on color differences, rather than as species names. The present study emphasizes the correctness of this usage because it shows that alurgite is essentially a muscovite that can attain a vivid color as a result of very small

Table 5. Comparison of structural parameters.

	Alurgite	Muscovite[1]	Manganophyllite[2]	Phlogopite-a[3]	Phlogopite-b[4]
a	5.2044 Å	5.1918 Å	5.316 Å	5.3141 Å	5.3078 Å
b	9.018	9.0153	9.221	9.2024	9.1901
c	20.073	20.0457	10.282	10.1645	10.1547
β	95.82°	95.735°	99.90°	100.05°	100.08°
Mean T(1)–O	1.644 Å	1.6445 Å	1.663 Å	1.6535 Å	1.649 Å
T(2)–O	1.644	1.644	—	—	—
τ T(1)	111.0°	110.9°	110.3°	110.6°	110.5°
T(2)	111.0	110.9	—	—	—
Rotation angle α	10.8°	11.3°	9.9°	7.7°	7.5°
Δz	0.22 Å	0.21 Å	0.01 Å	0.00 Å	0.00 Å
Thickness:					
Tet. sheet	2.243 Å	2.245 Å	2.266 Å	2.268 Å	2.261 Å
Interlayer sep.	3.393	3.393	3.454	3.356	3.352
Oct. sheet	2.106	2.089	2.143	2.116	2.125
Mean M(1)–O,OH,F	2.252 Å	2.241 Å	2.073 Å	2.066 Å	2.063 Å
M(2)–O,OH,F	1.934	1.930	2.072	2.063	2.064
Oct. distortions	62.1°	62.2°	58.9°	59.2°	59.0°
ψ M(1)	57.0	57.2	58.9	59.1	59.0
RMS M(1)[5]	7.2	7.3	3.9	4.2	4.1
M(2)	5.7	5.7	3.9	4.3	4.2
$(\sigma\theta)^2$ M(1)[6]	107.1	110.4	35.8	41.7	38.5
M(2)	58.5	59.0	36.0	42.2	39.7

[1] Rothbauer (1971).
[2] This study $(K_{0.84}Na_{0.07}Ba_{0.02})(Mg_{2.51}Fe^{3+}_{0.17}Mn^{2+}_{0.13}Al_{0.11}Ti_{0.01})(Si_{2.79}Al_{1.21})((OH)_{1.90}F_{0.10})O_{10}$.
[3] Joswig (1973) $(K_{0.90}Na_{0.02})(Mg_{2.71}Fe^{2+}_{0.26}Al_{0.08}Ti_{0.03})(Si_{2.91}Al_{1.09})((OH)_{0.97}F_{1.13})O_{10}$.
[4] Hazen and Burnham (1973) $(K_{0.77}Na_{0.16}Ba_{0.05})Mg_{3.00}(Si_{2.95}Al_{1.05})((OH)_{0.70}F_{1.30})O_{10}$.
[5] RMS octahedral distortion is defined as the rms-deviation of the 15 angles around the octahedral cations from their ideal values.
[6] $(\sigma\theta)^2$ is defined as $\sum_{i=1}^{12} (\theta_i - 90°)^2/11$, where θ_i is the observed O–M–O angle.

substitutions. A new species name would be appropriate only for a specimen in which octahedral Mn exceeded octahedral Al.

The causes of the color and pleochroism in pink to red muscovites have been attributed variously to the presence of Mn^{3+}, Fe^{3+}, or Ti^{3+} in octahedral and/or tetrahedral coordination (see, e.g., discussions by Richardson, 1975; Annersten and Hålenius, 1976; Richardson and Richardson, 1982). The alurgite of this study has a chemical composition nearly identical to that of the rose muscovite from Kenya studied by Richardson (1975) and Richardson and Richardson (1982), yet the colors are markedly different. Also, the Brazilian alurgite of this study shows normal pleochroism, whereas the Kenyan rose muscovite shows reverse pleochroism. Richardson (1975) attributed both the pink color and the reverse pleochroism of the Kenyan specimen to the presence of Fe^{3+} in tetrahedral sites. Richardson and Richardson (1982) refined the structure of the Kenyan specimen, but were unable to verify the presence of tetrahedral Fe^{3+}. Smith *et al.* (1983) used Mössbauer and optical spectra to explain reverse pleochroism in trioctahedral micas as due to absorption bands arising from transitions between energy levels of Fe^{3+}_{IV}-Mn^{2+}_{VI} ion pairs.

Manganophyllite

Calculated bond lengths and angles for manganophyllite are given in Table 4. Mean octahedral M–O,OH bond lengths of 2.073 and 2.072 Å for M(1) and M(2), respectively, indicate a disordered distribution of cations. The observed mean T–O bond length of 1.663 Å yields a tetrahedral composition of $Si_{0.66}Al_{0.34}$ upon application of the regression equation for micas of Hazen and Burnham (1973). This analysis is in good agreement with the microprobe analysis of $Si_{0.69}Al_{0.31}$.

Table 5 compares the cell dimensions, compositions, and several structural parameters of manganophyllite with those of two phlogopites whose structures have been determined accurately. Phlogopite-a (Joswig, 1972) and phlogopite-b (Hazen and Burnham, 1973) have similar compositions. This similarity shows up well in the closeness of their cell dimensions and structural parameters. The mean octahedral bond lengths and octahedral sheet thicknesses are about 0.02 Å smaller than expected for the octahedral composition of a hydroxy-phlogopite, however, because of the presence of substantial amounts of the smaller F in place of OH in both phlogopites. Manganophyllite has larger b and c repeats, larger mean M–O,OH,F distances, and

a larger octahedral sheet thickness than the two phlogopites because it has a low F content. All of these values are slightly smaller than those to be expected for a purely magnesian hydroxy-phlogopite, however, because of substitution of the smaller Fe^{3+}, Mn^{3+}, Al, and Ti for Mg in the octahedral sheet. Charge balance for these substitutions is achieved by substitution of more Al^{IV} for Si, thereby leading to greater lateral misfit of sheets and a larger tetrahedral rotation value. The greater interlayer separation is probably due to greater propping apart of adjacent layers by interaction between the interlayer cation and the hydrogen proton. Nevertheless, all of these differences are relatively small, and the manganophyllite structure compares well with that of phlogopite.

The hydrogen proton is 0.76 Å from the center of the OH group, where it is inclined at 85.6° to the *XY* plane. Giese's (1979) empirical formula predicts an inclination angle of 89.8°. The anisotropic thermal ellipsoids are comparable in size and orientation with those of alurgite (Table 3), with those of the basal oxygens elongate normal to the $T–O_b$ bonds.

ACKNOWLEDGMENTS

REFERENCES

Annersten, H. and Hålenius, U. (1976) Ion distribution in pink muscovite: a discussion: *Amer. Mineral.* **61**, 1045–1050.

Bilgrami, S. A. (1956) Manganese silicate minerals from Chikla, Bhandara district, India: *Mineral. Mag.* **31**, 236–244.

Burns, R. G. (1970) *Mineralogical Applications of Crystal Field Theory:* Cambridge University Press, Cambridge, Great Britain, 224 pp.

Cromer, D. T. and Mann, J. B. (1968) X-ray scattering factors computed from numerical Hartree-Fock wave functions: *Acta Crystallogr.* **A24**, 321–324.

Dollase, W. A. (1980) Optimum distance model of relaxation around substitutional defects: *Phys. Chem. Minerals* **6**, 255–304.

Fujino, K., Sasaki, S., Takéuchi, Y., and Sadanaga, R. (1981) X-ray determination of electron distribution in forsterite, fayalite and tephroite: *Acta Crystallogr.* **B37**, 513–518.

Gibbs, G. V. (1982) Molecules as models for bonding in silicates: *Amer. Mineral.* **67**, 421–450.

Giese, R. F., Jr. (1979) Hydroxyl orientations in 2:1 phyllosilicates: *Clays & Clay Minerals* **27**, 213–223.

Guggenheim, S. and Kato, T. (1984) Kinoshitalite and Mn phlogopites: trial refinements in subgroup symmetry and further refinement in ideal symmetry: *Mineral. J.* (Japan) **12**, 1–5.

Guggenheim, S., Schulze, W. A., Harris, G. A., and Lin, J-C. (1983) Non-centric layer silicates: an optical second harmonic generation, chemical, and X-ray study: *Clays & Clay Minerals* **31**, 251–260.

Hazen, R. M. and Burnham, C. W. (1973) The crystal structures of one-layer phlogopite and annite: *Amer. Mineral.* **58**, 889–900.

Hazen, R. M. and Wones, D. R. (1972) The effect of cation substitutions on the physical properties of trioctahedral micas: *Amer. Mineral.* **57**, 103–129.

Heinrich, E. W. (1946) Studies in the mica group; the biotite-phlogopite series: *Amer. J. Science* **244**, 836–848.

Heinrich, E. W. and Levinson, A. A. (1953) Mineralogy of the rose muscovites: *Amer. Mineral.* **38**, 25–49.

Heinrich, E. W. and Levinson, A. A. (1955) Studies in the mica group; polymorphism among the high-silica sericites: *Amer. Mineral.* **40**, 983–985.

Jakob, J. (1925) Beitrage zur chemischen Konstitution der Glimmer. I. Mitteilung: Die schwedischen Manganophylle: *Z. Kristallogr.* **61**, 155–163.

Joswig, W. (1972) Neutronenbeugungsmessungen an einem 1M-Phlogopit: *Neues Jahrb. Mineral. Monatshefte,* 1–11.

Penfield, S. L. (1893) On some minerals from the manganese mines of St. Marcel, in Piedmont, Italy: *Amer. J. Sci.* **46**, 288–295.

Richardson, S. M. (1975) A pink muscovite with reverse pleochroism from Archer's Post, Kenya: *Amer. Mineral.* **60**, 73–78.

Richardson, S. M. and Richardson, J. W., Jr. (1982) Crystal structure of a pink muscovite from Archer's Post, Kenya: implications for reverse pleochroism in dioctahedral micas: *Amer. Mineral.* **67**, 69–75.

Rothbauer, R. (1971) Untersuchung eines $2M_1$-Muskovits mit Neutronenstrahlen: *Neues Jahrb. Mineral. Monatshefte,* 143–154.

Sasaki, S., Fugino, K., Takéuchi, Y., and Sadanaga, R. (1980) On the estimation of atomic charges by the X-ray method for some oxides and silicates: *Acta Crystallogr.* **A36**, 904–915.

Smith, G., Hålenius, U., Annersten, H., and Ackermann, L. (1983) Optical and Mössbauer spectra of manganese-bearing phlogopites: Fe^{3+}_{IV}-Mn^{2+}_{VI} pair absorption as the origin of reverse pleochroism: *Amer. Mineral.* **68**, 759–768.

(Received 6 July 1985; accepted 1 October 1985; Ms. 1503)